Thin Solid Films xxx (2013) xxx–xxx

Contents lists available at SciVerse ScienceDirect

Thin Solid Films

journal homepage: www.elsevier.com/locate/tsf

Deformation localization in constrained layers of metallic glasses: A parametric modeling analysis

D.N. Rogers, Y.-L. Shen *

Department of Mechanical Engineering, University of New Mexico, Albuquerque, NM 87131, USA

ARTICLE INFO

Available online xxxx

Keywords:
Metallic glass
Thin film
Finite element analysis
Shear band
Plastic deformation

ABSTRACT

Localized plastic deformation known as shear banding is a prominent feature in metallic glasses. In this study we perform parametric three-dimensional finite element analyses, using primarily a thin layer of metallic glass on top of a cylindrical base, to study how physical constraint can affect this localized form of deformation and the corresponding macroscopic stress–strain response. Random perturbation points are added to the metallic glass model to facilitate the formation of shear bands. The modeling result suggests that the mechanical behavior of metallic glasses can be significantly influenced by the geometrical confinement. Under nominally uniaxial compressive loading, a lower thickness-to-diameter ratio results in higher plastic flow stresses. Shear bands tend to concentrate in regions away from the interface with the base material. The findings provide a mechanistic rationale for experimental observations based on the micropillar compression test. The deformation pattern in a multilayered metallic glass structure is also examined.

1. Introduction

The unique mechanical and functional properties displayed by bulk metallic glasses have sparked widespread interests in the materials research community [1–7]. These amorphous alloys generally exhibit elastic stiffness comparable to those of conventional engineering alloys, but their strengths at ambient temperature may be significantly higher. The absence of crystallinty in the microstructure, however, results in limited deformability. Dislocation slip, mechanical twinning and other deformation mechanisms associated with crystalline structures are no longer applicable. At below the glass transition temperature, plastic deformation occurs in a highly inhomogeneous manner via the formation and propagation of shear bands.

A shear band is typically a 10–100 nm-thick zone embedded within the relatively un-deformed matrix. Once shear starts locally, it tends to concentrate there and extends along a geometrically favorable path. In other words, the shear band becomes a weaker region than its surrounding. This is a manifestation of the *work softening* phenomenon inside a shear band. The accumulation of shear strain in an individual shear band may be as high as 10, although the overall ductility of the metallic glass specimen is still relatively small [8].

Metallic glasses in the form of deposited thin films have received great attention in recent years, due to their potential applications in emerging micro- and nano-scale devices [9,10]. As a result of their thin dimensions the flexibility can be improved, but deformation localization is still dominant once plastic yielding starts. In fact, the individual shear banding event may become more significant in affecting the mechanical property because of the small physical size. It has been reported that mechanical behavior of metallic glasses depends on their physical size [11–19]. While the atomic and structural origin of the intrinsic size effect has not been properly established, it is acknowledged that geometric confinement alone during mechanical testing of small-sized specimens can dictate the measured stress–strain response and deformation pattern in metallic glasses [10,20,21].

For traditional crystalline materials capable of homogeneous plastic deformation, the geometric confinement effect is well recognized. For instance, plastic deformation disturbed by physical constraint in small metallic structures (such as films, lines and joints), bonded to substrates or other adjoining materials, has been widely examined [22,23]. The same effect on materials showing inherently localized deformation such as shear banding, on the other hand, is in need of further investigations. The present study is thus devoted to externally constrained plasticity in metallic glasses from a numerical modeling standpoint. Parametric finite element analyses are performed, utilizing a modeling scheme of a thin layer of metallic glass on an underlying cylindrical base (representative of the micropillar compression test [10]). The primary objectives of this work include:

- To provide mechanistic insight into interface-mediated localized deformation, through a simple modeling strategy applied to uniaxial compressive loading;
- To explore the apparent yield strength and shear band evolution as affected by the aspect ratio of the metallic-glass thin films;
- To compare the constrained deformation behavior in materials prone to shear banding and traditional homogeneous plasticity.

* Corresponding author. Tel.: +1 505 277 6286.
E-mail address: shenyl@unm.edu (Y.-L. Shen).

0040-6090/$ – see front matter © 2013 Elsevier B.V. All rights reserved.
http://dx.doi.org/10.1016/j.tsf.2013.05.170

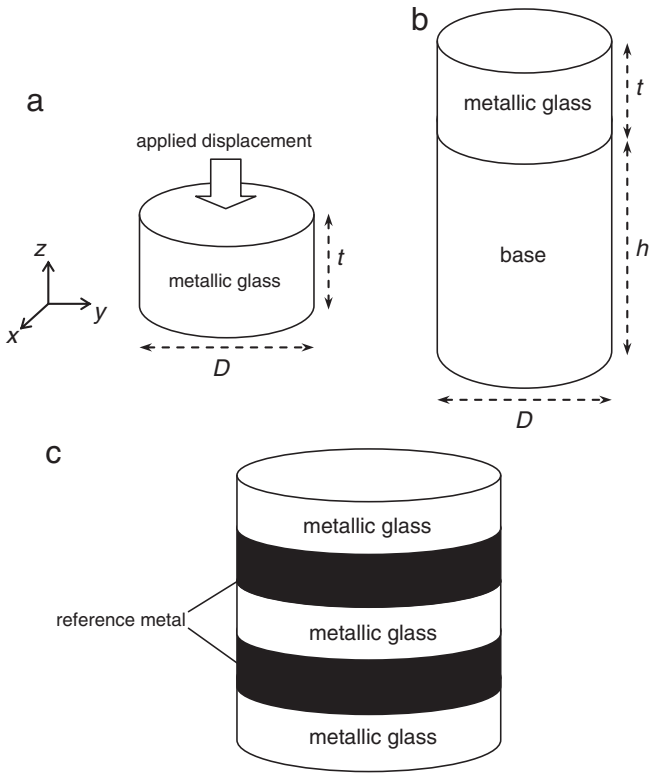

Fig. 1. Schematics of the numerical models subjected to compressive loading: (a) a stand-alone metallic glass cylinder, (b) a layer of metallic glass above a supporting base, and (c) multilayered metallic glass/reference metal structure.

Where applicable, qualitative comparisons with reported experimental observations are made and the implications discussed.

2. Numerical model

Three-dimensional finite element models were constructed. Fig. 1(a) shows a schematic of the model consisting of only the cylindrical metallic glass specimen itself. The diameter D is fixed at 1 μm, and various thickness (t) values from 0.2 to 1 μm are considered. Quasi-static compressive loading is applied through the prescribed displacement on the top face (initially at $z = t$). On the bottom face ($z = 0$), movement along the z-direction is prohibited but displacements in x and y are not constrained. This baseline case serves as a reference for contrasting

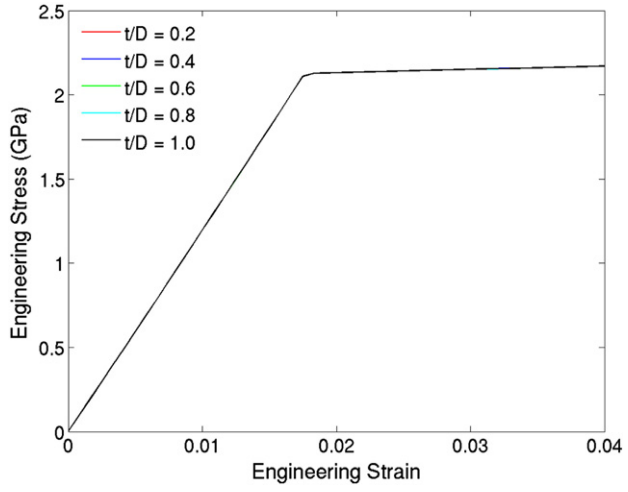

Fig. 2. Simulated compressive stress–strain curves for the stand-alone metallic glass cylinders, with aspect ratios 0.2, 0.4, 0.6, 0.8 and 1.0.

with other models involving a support material (substrate) as shown in Fig. 1(b). Here a metallic glass layer is attached to a base, and the entire structure is subject to compressive deformation. Two base materials, silicon (Si) and a hard metal (with hypothetical property described below), both with thickness (h) of 2 μm, are considered in this study. Fig. 1(c) shows another model with an alternating metallic glass/reference metal structure. The thickness of each layer is kept at 0.2 μm. This multilayered system provides an additional scenario for examining how the shear band formation may be affected by the physical constraint. Perfect bonding between dissimilar materials is assumed in all cases. The total number of elements in the simulations depends on the model type and actual geometry. As an example, in the case of $t = 1$ μm in Fig. 1(b), there are a total of 171,360 eight-noded linear hex elements. The finite element program Sierra/SolidMechanics (Sandia National Laboratories) was used in all calculations under the quasi-static condition.

All metallic materials in the model are treated as isotropic elastic-plastic solids. Young's modulus and Poisson's ratio of the metallic glass were taken to be 118 GPa and 0.37, respectively. Plastic yielding follows the von Mises criterion and incremental flow theory [24]. The choice of appropriate constitutive laws for amorphous alloys has been a topic of active research. Within the continuum framework, plasticity in crystalline metals is generally controlled only by the deviatoric part of the stress tensor. For disordered materials such as metallic glasses, hydrostatic pressure may be expected to influence the yield behavior. Pressure dependent plasticity models and their numerical implementation have been developed to simulate certain aspects of shear band formation in bulk metallic glasses [25–27]. On the other hand, many experimental investigations have concluded that the pressure dependence of plastic deformation is relatively weak (see Ref. [4] for discussion). Some studies specifically showed that the von Mises criterion is adequate for describing the yield response [28,29]. Therefore, for simplicity the von Mises criterion, with perfect plasticity upon yielding at a uniaxial stress of 2.1 GPa, is chosen for the present study. It is noted that the plasticity model alone is not able to capture the actual shear banding phenomenon. Rather, in the simulation we incorporated randomly generated "weak" points in the metallic glass to trigger discrete deformation along the maximum shear directions. The perturbation points, arbitrarily chosen to constitute 1% of the metallic glass elements unless otherwise stated, have the same elastic-plastic properties as the regular material elements, except for a built-in linear plastic work softening response of slope −18.9 GPa upon yielding. The softening stress–strain slope used in the model led to a decrease of stress to 10% within 0.1 strain. There will be no fundamental change in deformation pattern using different softening characteristics or different volumetric fractions of the perturbation points up to 10%. This is because the basic geometric features of strain localization stay unaffected. It is noted that the goal here is not to simulate the actual microscopic processes, but to induce a localized form of plastic flow in the model in a straightforward manner. A banded deformation pattern can be obtained with our current approach. The same numerical methodology has also been employed to elucidate the much improved bending ductility of a surface-coated bulk metallic glass [30].

The Si base in Fig. 1(b) is treated as a linear elastic solid, with Young's modulus and Poisson's ratio 107 GPa and 0.172, respectively. An alternative base material was also used; its elastic property is the same as the metallic glass and the yield strength is set at 4.2 GPa. Note that this "hard metal" base is a normal elastic-perfectly plastic solid with no mechanism built-in for deformation localization. As for the multilayer model in Fig. 1(c), the "reference metal" is also an elastic-perfectly plastic solid with the same elastic property. Its yield strength, however, is set to be 2.1 GPa which is equivalent to the initial yield point of the metallic glass. Therefore, the multilayer model may be viewed as a single metallic glass cylinder, but with two internal layers divested of the work softening (shear-band forming) capability.

Please cite this article as: D.N. Rogers, Y.-L. Shen, Deformation localization in constrained layers of metallic glasses: A parametric modeling analysis, Thin Solid Films (2013), http://dx.doi.org/10.1016/j.tsf.2013.05.170

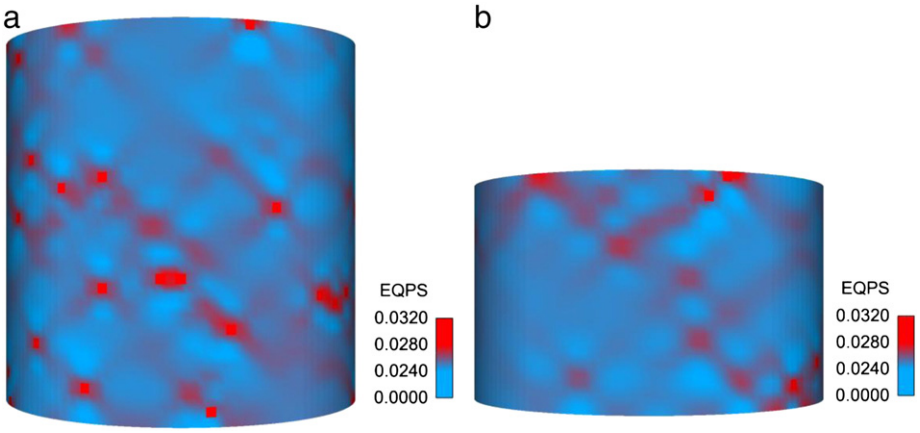

Fig. 3. Contours of equivalent plastic strain in the stand-alone metallic glass cylinders with aspect ratios (a) 1.0 and (b) 0.6, at the same macroscopic compressive strain of 0.042.

In the presentation below, simulated stress–strain curves of the metallic glass are obtained from the reaction force at each prescribed displacement, on the basis of the "engineering stress" and "engineering strain" definitions. In the case of base-supported pillar structure (Fig. 1(b)), the displacement of the base material was first subtracted from the total displacement so the true deformation in the metallic glass can be accounted for.

3. Results and discussion

3.1. Stand-alone metallic glass cylinder

Numerical results based on the model in Fig. 1(a) are first presented. Fig. 2 shows the simulated stress–strain curves of the metallic glass cylinders with various aspect ratios (defined to be t/D). It can be seen that, under uniaxial loading free of external constraint, the same stress–strain curves are obtained regardless of the geometry. Fig. 3(a) and (b) show the contour plots of equivalent plastic strain in the specimens with aspect ratios 1.0 and 0.6, respectively, when the overall compressive strain is 0.042. The localized deformation pattern is evident. Shear bands appear to be uniformly distributed throughout the material, and the plastic strains inside the bands are much greater than the surrounding. The extent of shear bands, in terms of both density and maximum plastic strain, for the two aspect ratios appears to be the same, which is consistent with the equivalence of overall stress–strain behavior observed in Fig. 2.

3.2. Cylinders constrained by base material

The substrate-supported pillar model in Fig. 1(b) is now considered. Fig. 4 shows the simulated stress–strain curves of the metallic glass cylinders when they are attached to a Si base. It is observed that different aspect ratios result in essentially the same elastic behavior. However, the plastic flow stress increases with decreasing aspect ratio. In other words, when the bottom face of the metallic glass is constrained by an elastic substrate, a shorter cylinder (becoming disk-like) will display a higher apparent mechanical strength. This is due to the decreasing volume that is relatively free to facilitate uninterrupted shear path along the 45° directions, as seen below.

Fig. 5 shows the yield stress as a function of aspect ratio of the metallic glass. Here the yield stress is defined to be the plastic flow stress at 1% offset strain. Note that this curve shows the same trend as in the pillar compression experiment [10,21]. When the aspect ratio is greater than about 0.5, the yield stress stays nearly constant. Below 0.5 a steep increase in yield stress is seen. Fig. 6(A) and (B) show the contour plots of equivalent plastic strain when the overall compressive strain of the metallic glass portion is at 0.042, in the models with aspect ratios of 1.0 and 0.6, respectively. It is notable that shear bands are more populated near the top of the specimen, away from the interface with Si. Plasticity is also much stronger in Fig. 6(A). Apparently the interfacial constraint, causing higher magnitudes of hydrostatic stress locally, tends to suppress plastic deformation in the metallic glass. Such an influence is thus greater in low-aspect-ratio models.

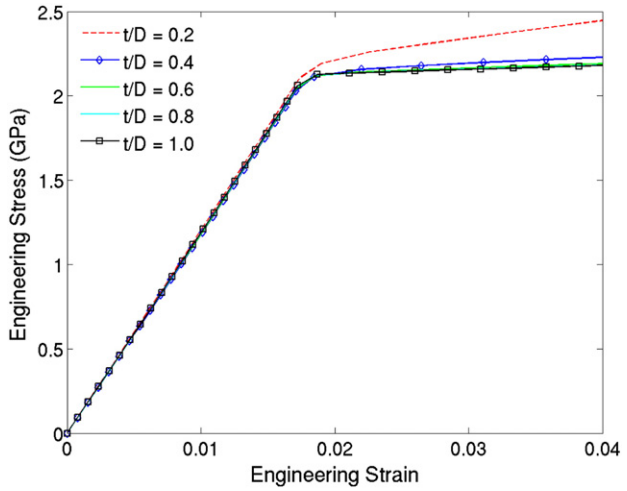

Fig. 4. Simulated compressive stress–strain curves for the metallic glass cylinders, with aspect ratios of 0.2, 0.4, 0.6, 0.8 and 1.0, when they are attached to a Si base.

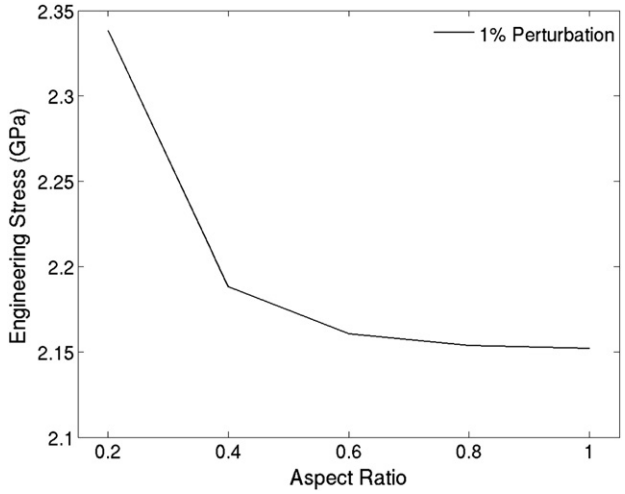

Fig. 5. Simulated 1% offset compressive yield stress as a function of the aspect ratio of the Si-attached metallic glass.

Please cite this article as: D.N. Rogers, Y.-L. Shen, Deformation localization in constrained layers of metallic glasses: A parametric modeling analysis, Thin Solid Films (2013), http://dx.doi.org/10.1016/j.tsf.2013.05.170

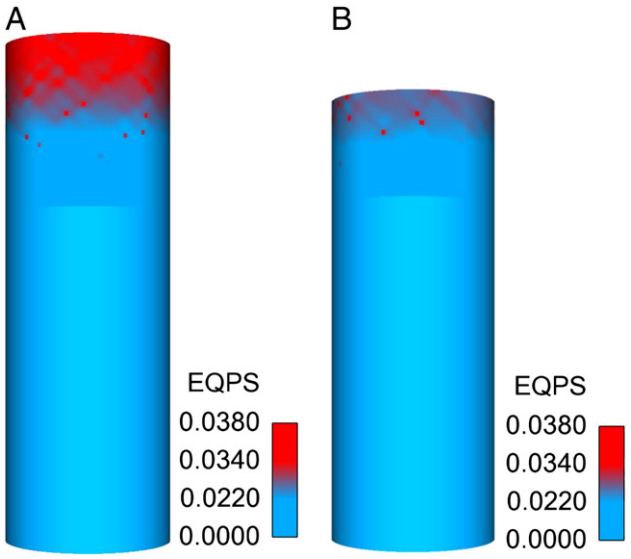

Fig. 6. Contours of equivalent plastic strain in the Si base-attached metallic glass cylinders with aspect ratios (A) 1.0 and (B) 0.6, at the same macroscopic compressive strain of 0.042.

To examine the possibly different effects of interfacial constraint on localized deformation as opposed to homogeneous deformation (traditional metal plasticity), we undertook a separate set of simulations using the same model configuration (Fig. 1(b)) but without the perturbation points that trigger shear bands. This means that the "metallic glass" under this special circumstance is simply an elastic-perfectly plastic material with the same elastic property and initial yield strength. Furthermore, we also included a case where an excessive number of perturbation points, namely 10% of the material elements, are incorporated into the metallic glass. It was found that these two additional cases lead to stress–strain curves similar to those in Fig. 4 (not shown here). When the simulated yield stress is plotted against the aspect ratio, Fig. 7, the same trend as in Fig. 5 is observed. The lower yield stress for the higher proportion of perturbation points is a consequence of more prominent work softening, while the overall trend with the aspect ratio remains unaffected. It is thus realized that the Si base-induced constraint influences the apparent strength of the metal cylinder in fundamentally the same way, irrespective of the localized or homogeneous form of deformation. It is worth mentioning that, in traditional metal plasticity, constrained

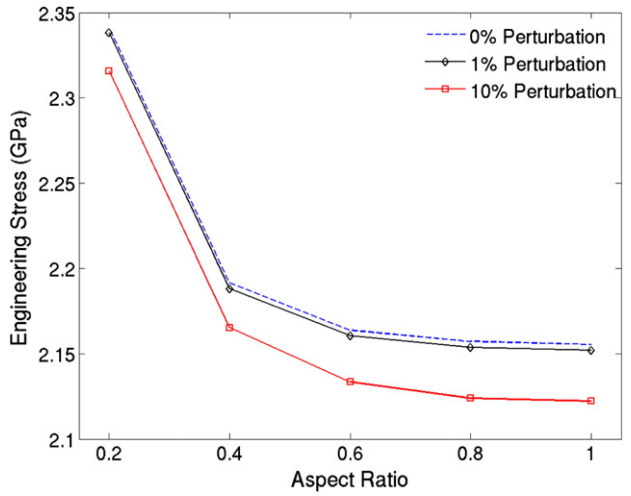

Fig. 7. Simulated 1% offset compressive yield stress as a function of the aspect ratio of the Si-attached metallic glass. In addition to the standard model of 1% perturbation points, two additional cases, with 0 and 10% perturbation points, are included.

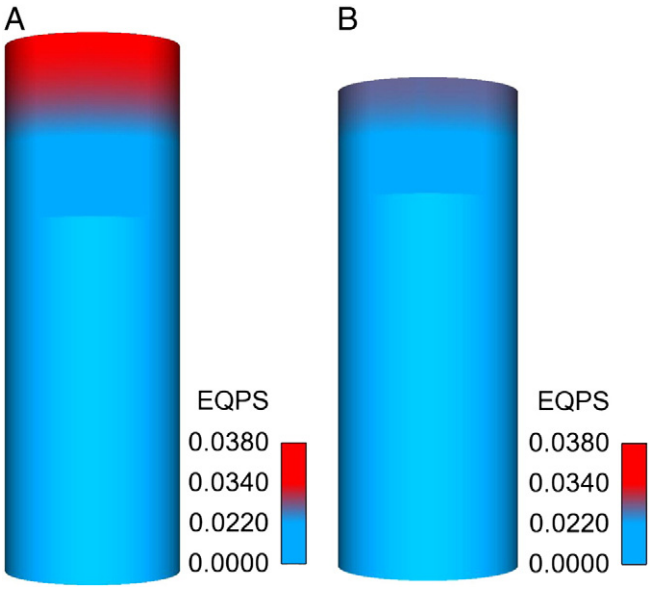

Fig. 8. Contours of equivalent plastic strain in the Si base-attached metallic glass free of any perturbation points, with aspect ratios (A) 1.0 and (B) 0.6, at the same macroscopic compressive strain of 0.042.

deformation is also dictated by the ease of flow along the 45° shear path [22,31,32].

Fig. 8(A) and (B) show the contour plots of equivalent plastic strain, in the case of an elastic-perfectly plastic "metallic glass" (no perturbation point) of aspect ratios of 1.0 and 0.6, respectively, when the macroscopic compressive strain of the metal portion is at 0.042. Although the material is capable of homogenous deformation, the interfacial constraint renders higher plastic strains near the top regions, especially in the higher-aspect-ratio model. Note that this observation has direct implications in interpreting experimental results of pillar compression for substrate-bonded *crystalline* metals. In the case of metallic glasses, the deformation pattern is manifested by the denser shear bands in the upper region and in the higher-aspect-ratio specimens (Fig. 6).

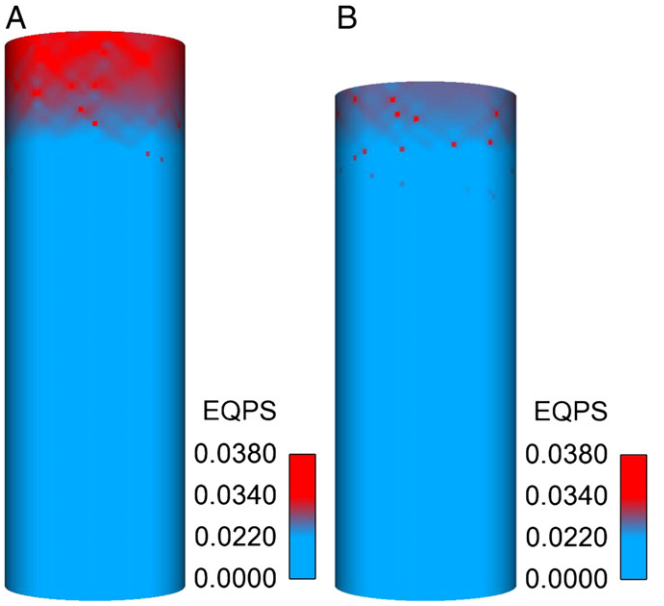

Fig. 9. Contours of equivalent plastic strain in the "hard metal" base-attached metallic glass cylinders with aspect ratios (A) 1.0 and (B) 0.6, at the same macroscopic compressive strain of 0.042.

Please cite this article as: D.N. Rogers, Y.-L. Shen, Deformation localization in constrained layers of metallic glasses: A parametric modeling analysis, Thin Solid Films (2013), http://dx.doi.org/10.1016/j.tsf.2013.05.170

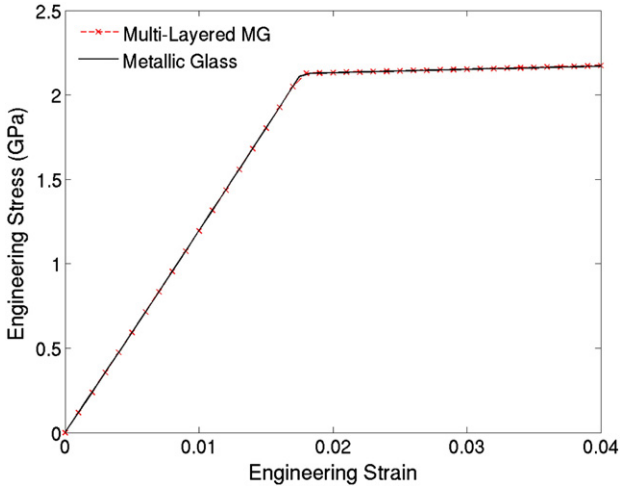

Fig. 10. Simulated compressive stress–strain curve of the multilayer model. Also included is the stand-alone metallic glass model of the same overall dimension (the case of $t/D = 1$ in Fig. 2).

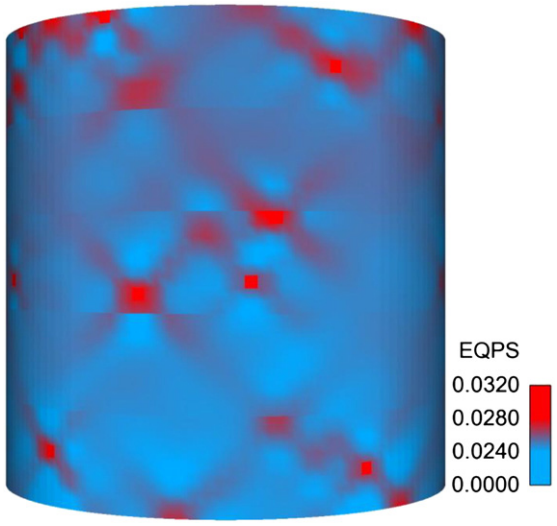

Fig. 11. Contour plot of equivalent plastic strain in the multilayer model when the macroscopic compressive strain is at 0.042.

In addition to the Si base, a "hard metal" base is also employed in this study. The "hard metal" is an elastic-perfectly plastic solid with a yield strength of 4200 MPa (much greater than the initial yield strength of the metallic glass). The standard constitutive model for the metallic glass described in Section 2 is used here. We seek to assess how the shear banding configuration in the metallic glass can be affected by a plastically deforming support structure. The result is presented in Fig. 9(A) and (B) where the contour plots of equivalent plastic strain corresponding to aspect ratios of 1.0 and 0.6, respectively, under the macroscopic compressive strain of 0.042 in the metallic glass portion, are shown. It can be seen, in comparison with the Si base in Fig. 6 under the same overall strain, that a hard but ductile base can allow slightly more shear bands developed in the metallic glass. Shear bands are still more populated in the upper region of the specimen. Since the base material also has the ability to plastically deform, the interface becomes less discernible in Fig. 9 compared to the case of an elastic Si base in Fig. 6.

To this end, it is noted that a ductile base with a yield strength lower than that of the metallic glass was also included in our preliminary study. Under this circumstance, plasticity mainly occurs in the base material rather than the metallic glass so the result is not presented here.

3.3. Multilayered structure

Attention is now turned to the multilayer model in Fig. 1(c). The "reference metal" sandwiched between the metallic glass layers is elastic-perfectly plastic, with the yield strength equal to the initial yield strength of the metallic glass. Fig. 10 shows the simulated stress–strain curves of the layered model and the all-metallic glass model of the same dimension (i.e., the curve of $t/D = 1$ in Fig. 2). The two curves essentially coincide. Fig. 11 shows the contour plot of equivalent plastic strain in the multilayer model, when the overall applied compressive strain is 0.042. While there is no perturbation point inside the reference metal, extension of shear bands from the adjacent metallic glass layers into the reference layers has occurred. By comparing Fig. 11 with Fig. 3(a), the insertion of reference metal layers is seen to cause discontinuity of localized deformation paths at the interfaces, and the overall shear band population and plastic heterogeneity are slightly reduced.

To further explore the effect of reference metal, we examined the same multilayer model but with reference metal having various strain hardening capabilities. All the other conditions remain unchanged. Fig. 12(A) and (B) show the contour plots of equivalent plastic strain at the overall applied compressive strain of 0.042, when linear plastic hardening slopes of 2.1 GPa and 21 GPa, respectively, were built into

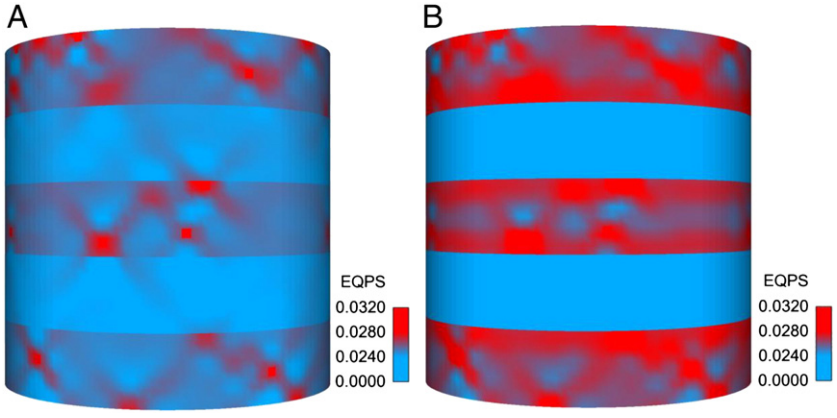

Fig. 12. Contour plots of equivalent plastic strain at the overall applied compressive strain of 0.042, when linear plastic hardening slopes of (A) 2.1 GPa and (B) 21 GPa, were built into the reference metal.

Please cite this article as: D.N. Rogers, Y.-L. Shen, Deformation localization in constrained layers of metallic glasses: A parametric modeling analysis, Thin Solid Films (2013), http://dx.doi.org/10.1016/j.tsf.2013.05.170

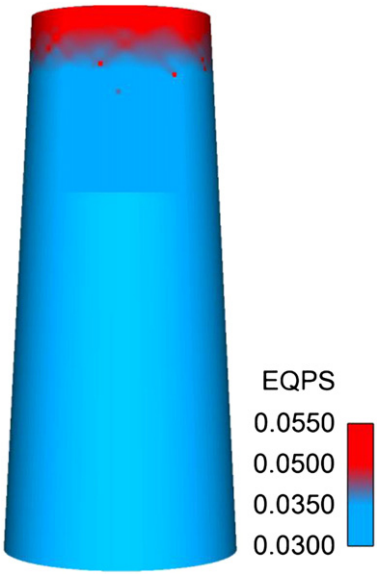

Fig. 13. Contour plot of equivalent plastic strain in the Si-base attached metallic glass model, with a 3° taper, at the macroscopic compressive strain of 0.042.

the reference metal. It can be seen in Fig. 12(A) that, compared to Fig. 11, the extension of shear bands into the hardening reference metal is notably reduced. In the case of higher strain hardening, Fig. 12(B), no localized deformation in the reference metal is seen. The much less deformable reference metal causes stronger deformation in the metallic glass layers, but the strain distribution tends to be more uniform, especially near the interfaces.

It is worth mentioning that multilayered pillars consisting of alternating metallic glass and other metal layers are also an active area of experimental research [33–35]. Shear bands initiated in the metallic glass films were found to be accommodated at the interface with the adjacent layer, which resulted in overall more homogeneous deformation and thus much improved ductility compared to monolithic metallic glass structures. The experimental findings are in qualitative agreement with the present discussion.

3.4. Effect of taper

In experiments, a slight taper is frequently seen in the FIB (focused ion beam)-fabricated micropillars. Here we utilize the model in Fig. 1(b) but with a 3° taper, and observe its deformation field. Fig. 13 shows the contour plot of equivalent plastic strain at the macroscopic compressive strain of 0.042, in the metallic glass of aspect ratio 1.0 above the Si base. It can be seen that localized deformation occurs primarily in the upper region away from the interface. In addition to the interfacial constraint, the smaller cross section area near the top boundary results in stress concentration, which also contributes to the inhomogeneous distribution of plastic strain. Constrained deformation due to physical confinement is thus further enhanced by the geometrical effect. The simulated deformation field is in line with carefully controlled experiments on Zr-, Mg- and Fe-based metallic glasses [36], where shear bands were all observed to nucleate from the top surface of the 2–4° tapered micropillars under compression. The taper geometry also plays an important role in affecting the measured pillar yield strength [36].

4. Conclusions

Systematic finite element analyses were conducted to study the evolution of shear bands in constrained metallic glass thin films. The models have the appearance of micropillars subject to compression, with or without a supporting base material, or with a multilayered configuration. Incorporation of randomized perturbation points in the model facilitated the localized plastic deformation. Without the influence of external constraint, the same stress–strain behavior and shear banding configuration can be obtained for stand-alone metallic glasses with various aspect ratios. When attached to a Si base (substrate), metallic glass cylinders with lower aspect ratios display higher plastic flow stresses. Shear bands are concentrated in the upper volume of the specimen, away from the interface with the base material. The effect is further enhanced if the cylinder shows a tapered geometry. The effect of aspect ratio on the apparent yield stress for base-attached metallic glasses follows the same trend as reported in experiment. The yield stress stays nearly constant if the aspect ratio is greater than 0.5. Furthermore, substrate-induced constraint is found to influence overall plastic deformation behavior in fundamentally the same way, regardless of the localized or homogeneous nature of the deformation. Forming multilayers by bonding thin-film metallic-glass with crystalline interlayers (with traditional plastic behavior) can potentially alleviate the strongly heterogeneous deformation configuration.

References

[1] A. Inoue, Acta Mater. 48 (2000) 279.
[2] J.F. Löffler, Intermetallics 11 (2003) 529.
[3] W.H. Wang, C. Dong, C.H. Shek, Mater. Sci. Eng. 44 (2004) 45.
[4] C.A. Schuh, T.C. Hufnagel, U. Ramamurty, Acta Mater. 55 (2007) 4067.
[5] M. Chen, Annu. Rev. Mater. Res. 38 (2008) 445.
[6] Y.Q. Cheng, E. Ma, Prog. Mater. Sci. 56 (2011) 379.
[7] A. Inoue, A. Takeuchi, Acta Mater. 59 (2011) 2243.
[8] M.A. Meyers, K.K. Chawla, Mechanical Behavior of Materials, Second edition Cambridge University Press, 2009.
[9] J.P. Chu, J.C. Huang, J.S.C. Jang, Y.C. Wang, P.K. Liaw, JOM 62 (4) (2010) 19.
[10] J.P. Chu, J.S.C. Jang, J.C. Huang, H.S. Chou, Y. Yang, J.C. Ye, Y.C. Wang, J.W. Lee, F.X. Liu, P.K. Liaw, Y.C. Chen, C.M. Lee, C.L. Li, C. Rullyani, Thin Solid Films 520 (2012) 5097.
[11] B.E. Schuster, Q. Wei, M.H. Ervin, S.O. Hruszkewycz, M.K. Miller, T.C. Hufnagel, K.T. Ramesh, Scripta Mater. 57 (2007) 517.
[12] C.J. Lee, J.C. Huang, T.G. Nieh, Appl. Phys. Lett. 91 (2007) 161913.
[13] H. Guo, P.F. Yan, Y.B. Wang, J. Tan, Z.F. Zhang, M.L. Sui, E. Ma, Nat. Mater. 6 (2007) 735.
[14] Z.W. Shan, J. Li, Y.Q. Cheng, A.M. Minor, S.A. Syed Asif, O.L. Warren, E. Ma, Phys. Rev. B 77 (2008) 155419.
[15] Y.H. Lai, C.J. Lee, Y.T. Cheng, H.S. Chou, H.M. Chen, X.H. Du, C.I. Chang, J.C. Huang, S.R. Jian, J.S.C. Jang, T.G. Nieh, Scripta Mater. 58 (2008) 890.
[16] C.A. Volkert, A. Donohue, F. Spaepen, J. Appl. Phys. 103 (2008) 083539.
[17] J.C. Ye, J. Lu, Y. Yang, P.K. Liaw, Acta Mater. 57 (2009) 6037.
[18] A. Bharathula, S.-W. Lee, W.J. Wright, K.M. Flores, Acta Mater. 58 (2010) 5789.
[19] Y. Yang, J.C. Ye, J. Lu, P.K. Liaw, C.T. Liu, Appl. Phys. Lett. 96 (2010) 011905.
[20] C.E. Packard, C.A. Schuh, Acta Mater. 55 (2007) 5348.
[21] J.C. Ye, J.P. Chu, Y.C. Chen, Q. Wang, Y. Yang, J. Appl. Phys. 112 (2012) 053516.
[22] Y.-L. Shen, Constrained Deformation of Materials, Springer, 2010.
[23] Y.-L. Shen, Prog. Mater. Sci. 53 (2008) 838.
[24] A. Mendelson, Plasticity: Theory and Application, MacMillan, New York, 1968.
[25] M. Zhao, M. Li, J. Mater. Res. 24 (2009) 2688.
[26] P. Thamburaja, R. Ekambaram, J. Mech. Phys. Solids 55 (2007) 1236.
[27] Y. Gao, Model. Simul. Mater. Sci. Eng. 14 (2006) 1329.
[28] H. Kimura, T. Masumoto, in: F.E. Lubrosky (Ed.), Amorphous Metallic Alloys, 1983, p. 87, (Butterworth).
[29] H.A. Bruck, T. Christman, A.J. Rosakis, W.L. Johnson, Scr. Metall. Mater. 30 (1994) 429.
[30] J.P. Chu, J.E. Greene, J.S.C. Jang, J.C. Huang, Y.-L. Shen, P.K. Liaw, Y. Yokoyama, A. Inoue, T.G. Nieh, Acta Mater. 60 (2012) 3226.
[31] Y.-L. Shen, M. Finot, A. Needleman, S. Suresh, Acta Metall. Mater. 43 (1995) 1701.
[32] Y.-L. Shen, Y.L. Guo, Model. Simul. Mater. Sci. Eng. 9 (2001) 391.
[33] M.C. Liu, C.J. Lee, Y.H. Lai, J.C. Huang, Thin Solid Films 518 (2010) 7295.
[34] H.S. Chou, X.H. Du, C.J. Lee, J.C. Huang, Intermetallics 19 (2011) 1047.
[35] S.Y. Kuan, H.S. Chou, M.C. Liu, X.H. Du, J.C. Huang, Intermetallics 18 (2010) 2453.
[36] J.C. Ye, J. Lu, Y. Yang, P.K. Liaw, Intermetallics 18 (2010) 385.

Please cite this article as: D.N. Rogers, Y.-L. Shen, Deformation localization in constrained layers of metallic glasses: A parametric modeling analysis, Thin Solid Films (2013), http://dx.doi.org/10.1016/j.tsf.2013.05.170